Low-temperature study of field-induced antiferromagnetic-ferromagnetic transition in Pd-doped Fe-Rh

Pallavi Kushwaha, Archana Lakhani, R. Rawat, and P. Chaddah
UGC-DAE Consortium for Scientific Research, University Campus, Khandwa Road, Indore 452001, India
(Received 8 June 2009; revised manuscript received 6 October 2009; published 17 November 2009)

The first-order antiferromagnetic (AFM) to ferromagnetic (FM) transition in the functional material $Fe_{49}(Rh_{0.93}Pd_{0.07})_{51}$ has been studied at low temperatures and high magnetic fields. We have addressed the nonmonotonic variation in lower critical field required for FM to AFM transition. It is shown that critically slow dynamics of the transition dominates below 50 K. At low temperature and high magnetic field, state of the system depends on the measurement history resulting in tunable coexistence of AFM and FM phases. By following cooling and heating in unequal magnetic field protocol it is shown that equilibrium state at 6 T magnetic field is AFM state. Glasslike FM state at 6 T (obtained after cooling in 8 T) shows reentrant transition with increasing temperature; viz., devitrification to AFM state followed by melting to FM state.

DOI: 10.1103/PhysRevB.80.174413 PACS number(s): 75.30.Kz, 72.15.Gd, 75.60.Nt

I. INTRODUCTION

Fe-Rh and its nearby compositions have been subject of extensive theoretical and experimental studies due to their various interesting magnetic properties.[1–11] As-prepared Fe-Rh order in fcc lattice, where Fe and Rh atoms are randomly distributed.[12] With annealing, it order in CsCl-type bcc structure, where Fe and Rh atoms occupy the corner and center positions of the cube, respectively. Magnetically, in the CsCl-type bcc structure, Fe-Rh shows a paramagnetic to ferromagnetic (FM) transition around $\approx 650-670$ K (T_C).[5,6] Magnetic moment of Fe and Rh atom in the FM state are reported to be $\approx 3.2\mu_B$ and $\approx 0.9\mu_B$, respectively.[7] With decreasing temperature, it shows a first-order FM to antiferromagnetic (AFM) transition. This transition is sensitive to Fe-Rh composition and preparation condition, therefore there is a large variation in FM to AFM transition temperature ($T_N \approx 320-370$ K) reported by various groups.[1,8–10] In the AFM state, there is no magnetic moment on Rh and the magnetic structure is type-II AFM, where ferromagnetic Fe layers (111) are coupled antiferromagnetically to each other.[7,11] This FM to AFM transition can also be influenced by the substitution of transition metal at Fe as well as Rh site.[1,6,13] Depending upon doping element (e.g., Ir, Pt, Pd, Ni, etc.) and concentration, T_N can be shifted (upward/downward) over a wide temperature range.[6] The origin of FM to AFM transition in this system is still debated. Since this transition is accompanied with an abrupt change in lattice parameter and unit-cell volume, Kittel exchange inversion model has been used to explain the transition.[14] However, this model fails to describe various features associated with this transition such as nonmonotonic variation in T_N with x in case of $Fe_{49}(Rh_{1-x}Pd_x)_{51}$,[1] anomalous entropy change, vanishing of Rh moment, etc.[1,15] Heat-capacity measurements show four times higher electronic contribution to heat capacity in FM state when compared to AFM state.[1,16,17] This led Annaorazov *et al.*[15] and Tu *et al.*[16] to suggested that band-structure modification as the origin of FM to AFM transition. On the other hand Chen *et al.*[18] reported small difference in the optical conductivity of FM and AFM phases through their ellipsometric studies. According to them, the low-temperature difference in heat capacity of AFM and FM state has magnetic origin rather than electronic origin. Density-functional calculations of Gu *et al.*[2] attributed the AFM-FM transition to the magnon (spin-wave) excitations. Besides the origin of the transition, interest in this system also arises due to their potential for technological applications. This is because FM to AFM transition is accompanied with large change in magnetization, resistivity, volume, etc., and transition can be influenced by magnetic field as well as pressure.[1,10,15,19,20] As a consequence giant magnetocaloric effect,[15,21] elastocaloric effect,[15] giant magnetoresistance,[10,13] magnetostriction,[22–24] etc., have been observed in this system. Multilayers of Fe-Rh/Fe-Pt films have been shown to form exchange spring system, which opens up the possibility for thermally assisted magnetic recording media.[3] Recently observation of laser-induced ultrafast switching between AFM and FM state on subpicoseconds time scale in Fe-Rh has opened another area of investigation.[4,25]

In spite of extensive investigations in this system, there are limited studies on the AFM-FM phases coexistence. Most of these studies are focused around room temperature or above, which is closed to T_N in the studied system. A detail magnetization (M) investigation of $Fe_{49}Rh_{51}$ thin films by Maat *et al.*[26] showed heterogeneous AFM to FM transition during warming irrespective of substrate. However FM to AFM transition upon cooling on c-axis sapphire substrate film suggested homogeneous nucleation and growth of AFM domain. This study also showed thermomagnetic irreversibility in M-H and M-T measurements arising due to supercooling and superheating associated with first-order transition. MFM study of Yokoyama *et al.*[27] showed inhomogeneous nucleation of FM domains at a micrometer length scale in $FeRh_{0.24}Pd_{0.76}$ and attributed to the internal stress caused by anisotropic lattice expansion at the transition. Manekar *et al.*[28] have studied the evolution of FM state in superheated AFM state by MFM in $Fe_{52}Rh_{48}$. They showed the coexisting AFM and FM phases in the sub-micrometer length scale and nucleation and growth of FM phase coupled with topography on a time scale of 10^4 s. On the other hand studies at low temperatures are rare in this system. Studies on fcc-structured nanoparticles of Fe-Rh showed spin-glass behav-

ior in magnetization measurement.[8,29] Baranov *et al.*[1] have carried out detailed studies of AFM-FM transition with various transition-metal doping down to 2 K. In $(Fe_{0.965}Ni_{0.035})_{49}Rh_{51}$ and $Fe_{49}(Rh_{0.92}Pd_{0.08})_{51}$, where the T_N is shifted to low temperature, they showed that critical field and hysteresis width follow T^2 and $T^{1/2}$ dependence, respectively. Below 5 K (for Ni) and 3.5 K (for Pd), they have noticed scattered but substantially lower hysteresis width (ΔH_c) and upper critical field (field required for AFM to FM transition) than the extrapolated curve obtained from high-temperature data. These features have been attributed to macroscopic quantum tunneling of magnetization through the energy barrier. Besides this, Figs. 2 and 5, and 8 of Baranov *et al.*[1] also reveal nonmonotonic variation in lower critical field showing a maxima at much higher temperature ($\approx$60 K). Similar kind of nonmonotonic variation in lower critical field has been shown and addressed in $Nd_{0.5}Sr_{0.5}MnO_3$ (Ref. 30) and $Mn_{1.85}Co_{0.15}Sb$.[31] There, such anomalous behavior has been explained in terms of critically slow dynamics of the transition on measurement time scale, which gives rise to glasslike arrested state (GLAS) at low temperature. In case of $La_{5/8-0.4}Pr_{0.4}Ca_{3/8}MnO_3$ (LPCMO) it has been shown that combination of glass transition temperature $T_G(H)$ and supercooling line $T^*(H)$ gives rise to nonmonotonic hysteretic boundary.[32] GLAS arises out of kinetic arrest of a first-order magnetic transition and is different from spin or cluster glass.[33,34] In analogy to structural glasses, GLAS shows devitrification on warming giving rise to large change in volume fraction of magnetic states.[33] GLAS and phase coexistence are of current interest particularly in manganites.[33] Therefore the study of first-order magnetic transition in Fe-Rh system provides an opportunity to check the universal feature of GLAS beyond manganites.

We have chosen $Fe_{49}(Rh_{0.93}Pd_{0.07})_{51}$ for the present study. This is because in $Fe_{49}(Rh_{1-x}Pd_x)_{51}$ system, T_N is reported to decrease from $\approx$350 K (x=0) to $\approx$180 K (x=0.08) and then increase again with increasing x before disappearing for $x \geq 0.13$.[1] Therefore T_N is minimum around $x \approx 0.08$. We carried out detailed magnetotransport studies on $Fe_{49}(Rh_{0.93}Pd_{0.07})_{51}$ which shows that dynamics of the transition becomes critically slow at low temperature and high magnetic field resulting in a nonmonotonic variation in lower critical field. It results in coexistence of glasslike arrested FM state and AFM state at low temperature. A cooling and heating in unequal field (CHUF) protocol[35] has been used to find out the equilibrium state of the system. This is the first study where critically slow dynamics of the transition is observed for AFM-FM transition accompanied with creation or vanishing of magnetic moment (on Rh).

II. EXPERIMENTAL DETAILS

The compound $Fe_{49}(Rh_{1-x}Pd_x)_{51}$ with x=0.07 was prepared by arc melting the constituent elements of purity better than 99.9% under high-purity argon atmosphere. Small pieces, cut from the same ingot, were wrapped in Tantulam foil and sealed in a quartz tube in $\approx 10^{-6}$ torr of vacuum and annealed at 900 °C for 20 h. For crystal structure analysis and phase detection, x-ray diffraction has been performed on polished surface of the ingot. The resistivity measurements were carried out by standard four-probe technique using a homemade resistivity setup with 8 T superconducting magnet system from Oxford Instruments Inc., UK. All the in-field measurements were performed in longitudinal geometry except isothermal magnetoresistance (MR) measurements, which were performed in transverse geometry up to 14 T using physical property measurement system (PPMS) from M/s. Quantum Design, USA. The MR is defined as MR $=\{\rho(H)-\rho(0)\}/\rho(0)$, where $\rho(0)$ is the resistivity in zero field and $\rho(H)$ is the resistivity in the presence of magnetic field H. Magnetization measurements were performed using vibrating sample magnetometer (VSM) option of PPMS.

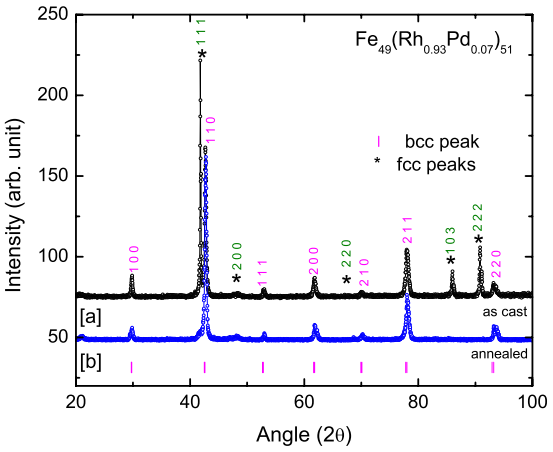

FIG. 1. (Color online) X-ray diffraction pattern for (a) as cast and (b) annealed sample. Peaks marked by stars (*)and vertical lines (|) correspond to fct- and CsCl-type bcc structure, respectively.

III. RESULTS AND DISCUSSION

Figure 1 shows the x-ray diffraction pattern of as cast and annealed $Fe_{49}(Rh_{0.93}Pd_{0.07})_{51}$. As cast sample is indexed by considering the presence of both fcc (it is fct with lattice parameters a and c almost equal) and bcc structure and corresponding peaks in the figure are marked by stars (*) and vertical lines (|), respectively. After annealing at 900 °C for 20 h, almost all of the fcc phase is converted into an ordered bcc structure. This observation is consistent with the earlier studies.[6,23]

Figure 2 shows the temperature dependence of resistivity for both the samples in the absence of magnetic field. As cast sample does not show any transition below room temperature but a difference between resistivity value during cooling and heating cycle is noticeable over entire temperature range. The origin of this hysteresis is not clear to us. This is similar to M-T measurement on Fe-Rh filings by Lommel *et al.*,[9] where magnetization at 300 K is smaller after cooling the sample to 78 K and warming back to 300 K. Annealed sample shows a sharp rise in resistivity with decreasing temperature which indicates transition from low-resistive FM phase to high-resistive AFM phase. During heating, a reverse transformation from AFM to FM state occurs at higher temperature resulting in a hysteresis, which is a signature of

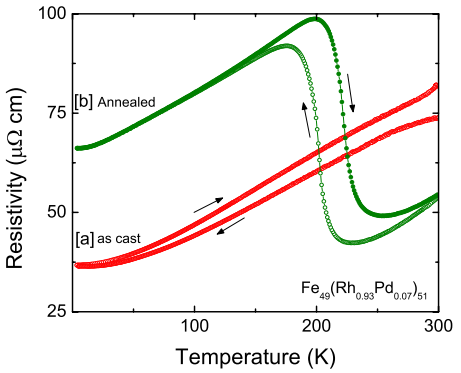

FIG. 2. (Color online) Resistivity behavior as a function of temperature for (a) as cast and (b) annealed sample. A first-order transition from FM (low-resistivity) to AFM (high-resistivity) state can be clearly seen in annealed sample.

first-order nature of the transition. The transition temperature, taken as the inflection point of the resistivity curve, is found to be ≈201 K during cooling and ≈222 K during heating. Besides this, FM to AFM transition is quite broad as transition width during cooling as well as heating is found to be around 55 K. The studies around T_N in analogous system has shown the presence of coexisting AFM and FM phases and broadening is attributed to residual lattice imperfection, chemical disorder along with the internal stress caused from anisotropic lattice expansion.[26–28] Due to disorder, different regions having length scale on the order of the correlation length can have different transition temperatures T_N, and this results in broadening of transition line as well as supercooling (T^*, H^*)/superheating (T^{**}, H^{**}) spinodals into a band for a macroscopic sample.[36] Since we are interested in the study of first-order AFM-FM transition at low temperature, further studies are performed on annealed sample only, which will be discussed in the following sections.

Figure 3 shows the temperature dependence of the resistivity in the presence of various constant magnetic fields. Labeled magnetic fields are applied isothermally at 300 K and data is recorded during cooling [field-cooled cooling (FCC)] and subsequent warming [field-cooled warming (FCW)]. Up to 4 T magnetic field, T_N decreases linearly (≈16 K/T) and both transition width (≈55 K) as well as hysteresis width (≈21 K) remains almost constant. This observation of constant hysteresis width with varying magnetic field is in agreement with the studies on analogous systems having T_N close to or above room temperature.[26] For 6 T magnetic field, transition width during cooling increases significantly in spite of decrease in resistivity jump across the transition. Since ρ value does not reach the zero-field resistivity value even after completion of hysteretic region, it suggests the presence of FM phase coexisting with AFM phase at low temperature. In the presence of 8 T magnetic field, there is no clear indication of FM-AFM transition, however, presence of small hysteresis indicates partial transformation of FM phase into AFM phase during cooling. These results show that with the application of magnetic field FM-AFM transition is suppressed only up to ≈50 K (instead of reducing toward 0 K) and no FM to AFM transformation takes place below this temperature. It is worth noting here that

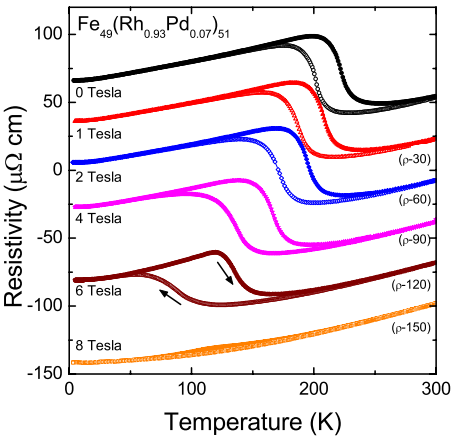

FIG. 3. (Color online) Temperature-dependent resistivity in different magnetic field conditions. Measurement has been performed during cooling (open symbol) and subsequent warming (solid symbol) in the presence of labeled magnetic field. Y axis is for 0 T curve. For the sake of simplicity, other curves are shifted downward by labeled value, e.g., label $(\rho-30)$ indicates that resistivity curve is shifted by 30 $\mu\Omega$ cm.

even transition-metal substitution studies show abrupt vanishing of AFM-FM transition temperature with substitution (or first-order transition with composition) and T_N is always found to be either higher than 100 K or absent.[1]

To verify if these coexisting states in 6 T and FM states in 8 T are ergodic state we followed different path for resistivity measurement under same temperature and magnetic field values as used in Fig. 3. Now, system is cooled to 5 K under zero field and labeled magnetic field applied isothermally at 5 K and resistivity is measured during warming [zero-field-cooled warming (ZFCW)]. Figure 4 shows ZFCW curves along with corresponding FCW curves taken from Fig. 3. For

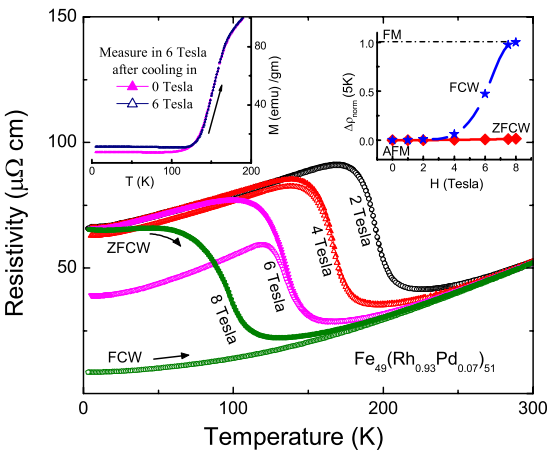

FIG. 4. (Color online) Resistivity vs temperature in the presence of labeled magnetic field measured during warming. ZFCW curves were measured after cooling in zero-field and FCW curves were measured after cooling in same field value. The left inset shows the temperature dependence of magnetization in the presence of 6 T magnetic field. The right inset shows $\Delta\rho_{norm}$ at 5 K for FCW (star) and ZFCW (diamond) curve, highlighting the path dependence of FM and AFM phase fraction (see text for details).

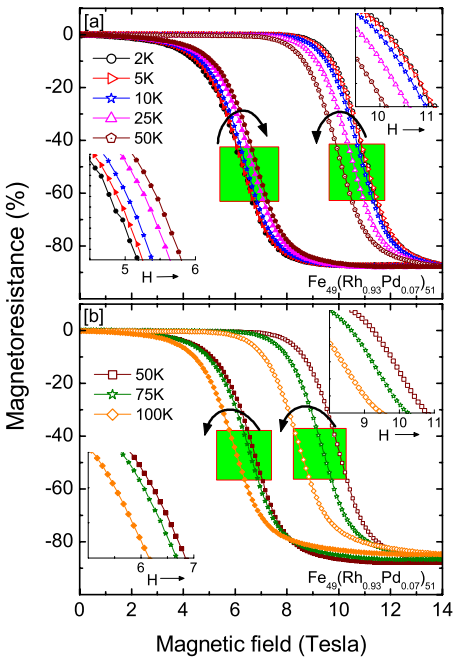

FIG. 5. (Color online) The magnetic field dependence of resistivity at various constant temperatures are shown in (a) below 50 K and (b) above 50 K. Increasing and decreasing magnetic field cycles are denoted by open and solid symbols, respectively. Upper right insets of both the graphs show the enlarged section of increasing field cycle whereas lower left inset correspond to decreasing field cycle. The forward curves ($0 \rightarrow 14$ T) move to lower-field values monotonically with increasing temperature ($5 \rightarrow 100$ K) as highlighted by the curved arrows. Whereas, the reverse curves (14 T $\rightarrow 0$) move nonmonotonically with temperature. Below/above 50 K, it shifts to higher/lower-field value with increasing temperature as highlighted by oppositely directed curved arrow in figures (a) and (b), respectively.

2 and 4 T both the curves are almost identical. However for 6 and 8 T, ZFCW curves have higher resistivity compared to FCW curve below T_N. Left inset of Fig. 4 shows the ZFCW and FCW magnetization curves in the presence of 6 T magnetic field. The finite magnetization in presence of 6 T after ZFC is arising due to susceptibility of antiferromagnetic phase.[22] FCW curve shows higher magnetization compared to ZFCW. A difference between ZFCW and FCW in magnetization measurement has been observed by Navarro *et al.*[8] and Hernando *et al.*[29] on ball-milled fcc Fe-Rh. There the difference between ZFCW and FCW decreases with increasing magnetic field and is attributed to spin-glass behavior. However in our case, the difference between ZFCW and FCW increases with increasing magnetic field (but less than critical field required for AFM-FM transition at 5 K) which rules out the presence of spin glass. The difference between ZFCW and FCW curves reduces as the applied field becomes higher than 9 T because the isothermal AFM to FM transition starts at 5 K, as shown in the R vs H curve in Fig. 5(a). Consequently, at 14 T, system will be in FM state along ZFCW curve also. These thermomagnetic irreversibility for resistivity in ZFCW and FCW curves are similar to that observed across disorder broadened first-order magnetic transition in many other systems such as doped $CeFe_2$,[33] $Nd_{0.5}Sr_{0.5}MnO_3$,[30] $Mn_{1.85}Co_{0.15}Sb$, etc.[31] There it has been attributed to critically slow dynamics of the transition due to which high-temperature phase remains arrested down to the lowest temperature. To have some estimate of the FM-phase fraction at 5 K we assumed that resistivity decreases linearly with increasing FM-phase fraction and the resistivity values corresponding to FM state (ρ_{FM}) and AFM state (ρ_{AFM}) are taken as the 8 T FCW curve and 0 T (zero-field-cooled) curve resistivities at 5 K, respectively. With this assumption the quantity $\Delta\rho_{norm}[=\{\rho_{\mathrm{AFM}}-\rho(H,T)\}/\{\rho_{\mathrm{AFM}}-\rho_{\mathrm{FM}}\}]$ gives FM-phase fraction at temperature T and magnetic field H. Obtained $\Delta\rho_{norm}$ at 5 K is shown as inset of Fig. 4 for both ZFCW and FCW curves. For ZFCW curve $\Delta\rho_{norm}$ remains zero for all the field values which indicates that the system is in homogeneous AFM state at 5 K and applied magnetic field is not sufficient enough to induce AFM to FM transition. Whereas, in case of FCW curve it deviates from ZFCW curve for $H \geq 6$ T that shows increased FM-phase fraction with increasing magnetic field. In case of 6 T, it indicates coexisting AFM and FM phases and the state of the system depends on the path followed in H-T space. On the other hand we could obtain almost homogeneous AFM or FM state in presence of 8 T magnetic field depending on the cooling history.

Since the isothermal application of 8 T magnetic field at 5 K does not show any field-induced AFM-FM transition for a zero-field-cooled sample, we used PPMS for measurement up to 14 T to study this transition isothermally below T_N. These measurements were carried out in transverse geometry. We cross checked results of these measurements with the measurement of longitudinal geometry using 8 T magnet system. We found similar behavior in both the geometries except slightly higher MR magnitude ($\approx 4\%$) and higher critical field (difference ≈ 0.5 T) in transverse geometry though the trend remains same. For these isothermal MR measurement, sample was cooled under zero field from well above T_N to the lowest temperature (2 K) of the measurement. All the measurements have been done during subsequent warming in such a way that the every next-higher temperature measurement was performed after completion of previous low-temperature measurement. The results of these measurements are shown in Fig. 5. With the application of magnetic field, a field-induced transition from AFM to FM phases is observed as a sharp change in MR. For all the temperatures, giant MR $\approx 90\%$ is observed across AFM to FM transition. The reverse transformation occurs at lower-field value resulting in a hysteretic field dependence of MR. During decreasing magnetic field, system recovers its initial resistivity value at 0 T, which indicates complete reverse transformation from FM to AFM phase. This high MR is observed when system is prepared under zero-field condition and magnetic field is cycled back to zero. Whereas in Fig. 4 it has been shown that if the sample is prepared in FC state same large MR would not be observed. The right insets of Figs. 5(a) and 5(b) shows that with increasing temperature, forward ($0 \rightarrow 14$ T) curves shift monotonically to lower-field side. However the return curves ($14\ \mathrm{T} \rightarrow 0$) shift to higher-field side up to 50 K [left corner inset of Fig. 5(a)] and then to lower-field side [left corner inset of Fig. 5(b)] with increasing temperature. This behavior is similar to that ob-

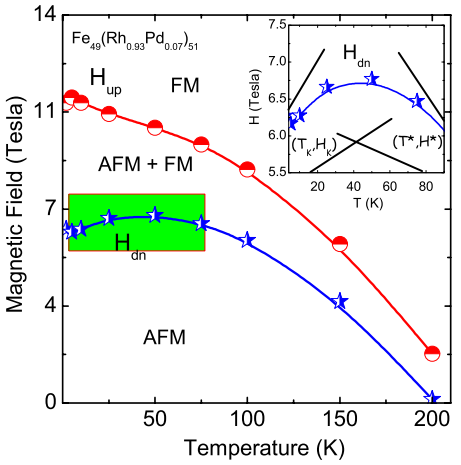

FIG. 6. (Color online) *H-T* phase diagram obtained from isothermal MR measurements shown in Fig. 5. Inset highlights the nonmonotonic variation in lower critical field and straight lines represent (H_K,T_K) and (H^*,T^*) bands schematically.

served in $Nd_{0.5}Sr_{0.5}MnO_3$, where it is attributed to dominance of critically slow dynamics of the transition below 60 K.[30]

The variation in critical fields is more explicitly demonstrated in *H-T* phase diagram (Fig. 6) which is obtained from isothermal magnetoresistance shown in Fig. 5. H_{up} (critical field required for AFM to FM transition) and H_{dn} (critical field required for FM to AFM transition) are taken as inflection point of MR vs H curve during increasing and decreasing magnetic field, respectively. This phase diagram shows that curve corresponding to H_{up} varies monotonically with temperature whereas H_{dn} varies nonmonotonically with a shallow maxima around 50 K (see inset of Fig. 6). Nonmonotonic variation in lower critical field is addressed in $Nd_{0.5}Sr_{0.5}MnO_3$ (Ref. 30) and $Mn_{1.85}Co_{0.15}Sb$ (Ref. 31) in terms of interplay between transformation kinetics and supercooling. This interplay is highlighted schematically in the inset of Fig. 6 for the present system. At low-temperature [below (H_K,T_K)] dynamics of the transition becomes critically slow and wins over thermodynamic transition. Since dynamics of the transition dominates at low temperature, H_{dn} is determined by (H_K,T_K) in this temperature region, in contrast to high temperature where it is determined by (H^*,T^*). Therefore the positive slope region is representative of (H_K,T_K) and the negative slope region is representative of (H^*,T^*). With this understanding of phase diagram it is obvious that transition field at which the free energy of both the FM and AFM states becomes equal will be higher than the middle point of H_{up} and H_{dn} at low temperatures. Nonmonotonic variation in critical field is common in manganites where such glassy magnetic states are being extensively studied. In case of LPCMO where high-temperature state is AFM-charge order, Wu *et al.*[32] have identified this kinetic arrest line (H_K,T_K) as T_G (glass transition) line.

So far we have shown that interplay of (H_K,T_K) and (H^*,T^*) give rise to coexisting AFM and FM phases at low temperature and the phase fraction depends on the path followed in *H-T* phase space. Now question arises, which of these phases is the equilibrium phase. For this, CHUF

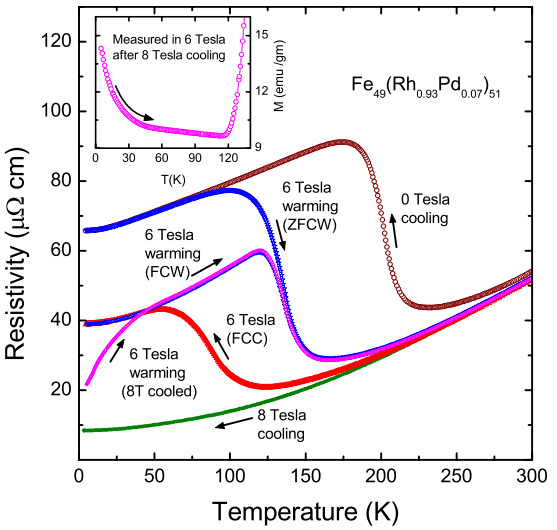

FIG. 7. (Color online) Resistivity as a function of temperature using CHUF protocol. Sample is cooled under different magnetic field of 0, 6, and 8 T, respectively, whereas measurement during warming are carried out in 6 T only. A reverse transformation from arrested FM to AFM at low temperature is clearly seen during heating in 6 T after 8 T field cooling only. The usual first-order AFM to FM transition is visible for all the warming curve for different field cooling. Inset shows the magnetization measured in the presence of 6 T magnetic field during warming after field cooling in the presence of 8 T magnetic field.

protocol[35] is used, the results of which are shown in Fig. 7. Under this protocol, measurements during warming are carried out under a constant magnetic field after cooling the sample in the presence of different magnetic fields. If high-field state happens to be nonequilibrium state then for cooling field higher than measuring field one observes a double (reentrant) transition and for smaller cooling field there will be only one transition. For the present system we cooled the system in the presence of 0, 6, and 8 T field to 5 K. At 5 K, magnetic field is changed isothermally to 6 T and then measurement is performed during warming in the presence of 6 T magnetic field. The resistivity value at 5 K and 6 T depends on the cooling field, which shows the tunability of AFM/FM phase fraction. Cooling in higher-field results in higher FM-phase fraction. When the cooling field (0 T) is lower then warming field (6 T), system shows only one transition, i.e, transformation from AFM to FM state around 125 K. Whereas two transitions appear when cooling field (8 T) is higher than measuring field (6 T). Corresponding magnetization curve (cooled in 8 T and measured in 6 T warming) in the inset of Fig. 7 also shows two transitions. It shows that low-field state (here AFM) is equilibrium phase and FM phase exist as glasslike arrested phase. During warming in 6 T (after cooling in 8 T) an increase/decrease in the resistivity/magnetization at low temperature indicates devitrification of glasslike FM phase into AFM phase. The reentrant transition, corresponding to melting of AFM phase in to FM phase, is seen by a sharp fall/rise in resistivity/magnetization after crossing superheating band with further increase in the temperature.

These results show that cooling in high magnetic field results in glasslike FM state as the FM state obtained in this

way remains arrested until system crosses (H_K, T_K) band on lowering the magnetic field isothermally (see Fig. 5). The origin of glasslike arrested magnetic state is debatable even in manganites, where it has been subject matter of extensive investigation in recent years. Like manganites, there is a delicate balance between AF and FM interaction in Fe-Rh system. This can be seen in Fig. 2, where we observe a sharp transition in annealed (chemically ordered) sample in contrast to broad features observed in the as cast sample. Not only this band structure in AFM and FM states are shown to be different. Therefore there are strong coupling between magnetic, electronic, and lattice degrees of freedom, and AFM-FM transition is sensitive to disorder, strain, etc. In case of LPCMO Sharma *et al.*[33] has linked the glass formation to freezing of structural degrees of freedom. According to them potential mechanism for glass formation lies in the first-order structural phase transition. In the present system also AFM-FM transition is accompanied with large lattice volume change though the crystal structure symmetry remains same. The magnetic force microscopy (MFM) study of Manekar *et al.*[28] around room temperature in Fe-Rh system has shown the growth of FM phase correlated with topology on a time scale of 10^4 s. We would like to caution here that the driving mechanism (lattice or magnetic) for first-order transition in this system is yet to be identified. When the transition is shifted to lower temperature (in the present system achieved by Pd doping and applying magnetic field) the atomic motion is hindered at low temperature due to lower thermal energy. The effect of Pd doping appears to be similar to metallic glass where melting temperature (but not glass transition temperature) is found to be strong function of composition.[37] In fact even in the case of LPCMO thin film grown on different substrate, glass transition temperature appears to be less sensitive to substrate strain in comparison to AFM-FM transition temperature.[38]

IV. CONCLUSIONS

To conclude we have studied first-order AFM to FM transition at low temperature using detailed magnetotransport studies on $Fe_{49}(Rh_{0.93}Pd_{0.07})_{51}$. Similar to abrupt vanishing of T_N with transition-metal doping,[1] these studies show gradual decrease in transition temperature but only down to 50 K and absence of AFM-FM transition below this temperature. Nonmonotonic variation in H_{dn} observed in isothermal MR measurement has been explained by the interplay of (H_K, T_K) and (H^*, T^*) bands. At low temperature and high magnetic field, state of the system depends on the measurement history and can give rise to coexisting AFM and FM states. Nature of coexisting AFM and FM phases has been studied by following novel paths in *H-T* space which shows FM state as GLAS and its devitrification with increasing temperature. The observed glasslike features in the studied system are similar to glassy magnetic states observed in manganites and related systems. The applicability of the concepts developed in these studies to the present system shows universality. Further microscopic studies will be helpful in understanding the glassy behavior in these systems.

ACKNOWLEDGMENTS

We thank N. P. Lalla, R. J. Choudhary, and Suresh Bhardwaj for XRD measurements, V. Ganesan and Swati Pandya for isothermal magnetoresistance measurements, Alok Banerjee and Kranti Kumar for magnetization measurements. DST, government of India is acknowledged for funding the PPMS and VSM-PPMS used in the present study. Pallavi Kushwaha acknowledges CSIR, India for financial support.

[1] N. V. Baranov and E. A. Barabanova, J. Alloys Compd. **219**, 139 (1995).
[2] R. Y. Gu and V. P. Antropov, Phys. Rev. B **72**, 012403 (2005).
[3] Jan-Ulrich Thiele, Stefan Maat, and Eric E. Fullerton, Appl. Phys. Lett. **82**, 2859 (2003); K. Yu. Guslienko, O. Chubykalo-Fesenko, O. Mryasov, R. Chantrell, and D. Weller, Phys. Rev. B **70**, 104405 (2004).
[4] G. Ju, J. Hohlfeld, B. Bergman, R. J. M. van deVeerdonk, O. N. Mryasov, J.-Y. Kim, X. Wu, D. Weller, and B. Koopmans, Phys. Rev. Lett. **93**, 197403 (2004).
[5] J. S. Kouvel and C. C. Hartelius, J. Appl. Phys. **33**, 1343 (1962).
[6] J. S. Kouvel, J. Appl. Phys. **37**, 1257 (1966).
[7] G. Shirane, C. W. Chen, P. A. Flinn, and R. Nathans, J. Appl. Phys. **34**, 1044 (1963); G. Shirane, R. Nathans, and C. W. Chen, Phys. Rev. **134**, A1547 (1964).
[8] E. Navarro, M. Multigner, A. R. Yavari, and A. Hernando, Europhys. Lett. **35**, 307 (1996).
[9] J. M. Lommel and J. S. Kouvel, J. Appl. Phys. **38**, 1263 (1967).
[10] P. A. Algarabel, M. R. Ibarra, C. Marquina, A. del Moral, J. Galibert, M. Iqbal, and S. Askenazy, Appl. Phys. Lett. **66**, 3061 (1995).
[11] V. L. Moruzzi and P. M. Marcus, Phys. Rev. B **46**, 2864 (1992).
[12] C. C. Chao, P. Duwez, and C. C. Tsuei, J. Appl. Phys. **42**, 4282 (1971).
[13] N. V. Baranov, P. E. Markin, S. V. Zemlyanski, H. Michor, and G. Hilscher, J. Magn. Magn. Mater. **157-158**, 401 (1996).
[14] C. Kittel, Phys. Rev. **120**, 335 (1960).
[15] M. P. Annaorazov, S. A. Nikitin, A. L. Tyurin, K. A. Asatryan, and A. Kh. Dovletov, J. Appl. Phys. **79**, 1689 (1996).
[16] P. Tu, A. J. Heeger, J. S. Kouvel, and J. B. Comly, J. Appl. Phys. **40**, 1368 (1969).
[17] J. Ivrsson, G. R. Pickett, and J. Toth, Phys. Lett. **35A**, 167 (1971).
[18] L. Y. Chen and D. W. Lynch, Phys. Rev. B **37**, 10503 (1988).
[19] M. Rajagopalan, Int. J. Mod. Phys. B **19**, 3389 (2005).
[20] R. C. Wayne, Phys. Rev. **170**, 523 (1968).
[21] M. P. Annaorazov, H. M. Guven, and K. Barner, J. Alloys Compd. **397**, 26 (2005).
[22] J. A. Ricodeau and D. Melville, J. Phys. (France) **35**, 149 (1974).
[23] M. R. Ibarra and P. A. Algarabel, Phys. Rev. B **50**, 4196 (1994).
[24] C. Marquina, M. R. Ibarra, P. A. Algarabel, A. Hernando,

P. Crespo, P. Agudo, A. R. Yavari, and E. Navarro, J. Appl. Phys. **81**, 2315 (1997).

[25] J.-U. Thiele, M. Buess, and C. H. Back, Appl. Phys. Lett. **85**, 2857 (2004)

[26] S. Maat, J.-U. Thiele, and Eric E. Fullerton, Phys. Rev. B **72**, 214432 (2005).

[27] Y. Yokoyama, M. Usukura, S. Yuasa, Y. Suzuki, H. Miyajima, and T. Katayama, J. Magn. Magn. Mater. **177-181**, 181 (1998).

[28] M. Manekar, C. Mukhaerjee, and S. B. Roy, Europhys. Lett. **80**, 17004 (2007).

[29] A. Hernando, E. Navarro, M. Multigner, A. R. Yavari, D. Fiorani, M. Rosenberg, G. Filoti, and R. Caciuffo, Phys. Rev. B **58**, 5181 (1998).

[30] R. Rawat, K. Mukherjee, K. Kumar, A. Banerjee, and P. Chaddah, J. Phys.: Condens. Matter **19**, 256211 (2007).

[31] Pallavi Kushwaha, R. Rawat, and P. Chaddah, J. Phys.: Condens. Matter **20**, 022204 (2008).

[32] W. Wu, C. Israel, N. Hur, P. Soonyong, S.-W. Cheong, and A. De Lozane, Nature Mater. **5**, 881 (2006).

[33] S. B. Roy, P. Chaddah, V. K. Pecharsky, and K. A. Gschneidner, Jr., Acta Mater. **56**, 5895 (2008); P. A. Sharma, S. El-Khatib, I. Mihut, J. B. Betts, A. Migliori, S. B. Kim, S. Guha, and S.-W. Cheong, Phys. Rev. B **78**, 134205 (2008).

[34] S. B. Roy and M. K. Chattopadhyay, Phys. Rev. B **79**, 052407 (2009).

[35] A. Banerjee, Kranti Kumar, and P. Chaddah, J. Phys.: Condens. Matter **21**, 026002 (2009).

[36] Y. Imry and M. Wortis, Phys. Rev. B **19**, 3580 (1979); Kranti Kumar, A. K. Pramanik, A. Banerjee, P. Chaddah, S. B. Roy, S. Park, C. L. Zhang, and S.-W. Cheong, *ibid.* **73**, 184435 (2006).

[37] A. L. Greer, Science **267**, 1947 (1995).

[38] V. G. Sathe, Anju Ahalawat, R. Rawat, and P. Chaddah (private communication).